Deconvolution of Spatial Transcriptomics Using scRNA-seq

Wenxin Jiang

Oct. 18, 2024

How to Use This Webpage

Click the button at the lower left to open the menu.

Press esc on your keyboard to enter navigation mode.

Press ? on your keyboard to view keyboard shortcuts.

Structure of the Presentation

1. Introduction to spatial transcriptomics and scRNA-seq
2. Deconvolution methods: RCTD and Cell2Location
3. Comparison: Simulation and Real data

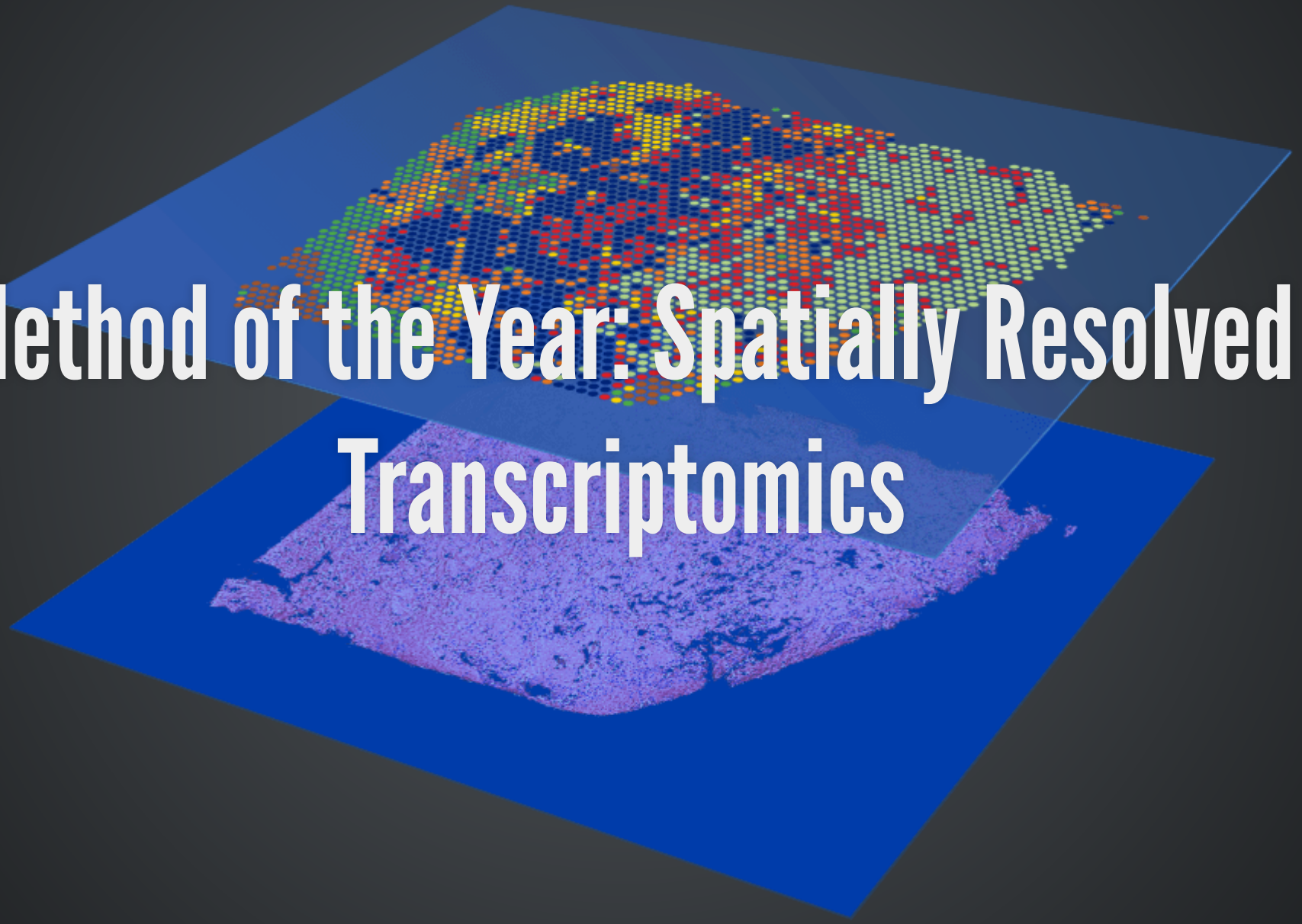

Method of the Year: Spatially Resolved Transcriptomics

Comparison between Sequencing Methods

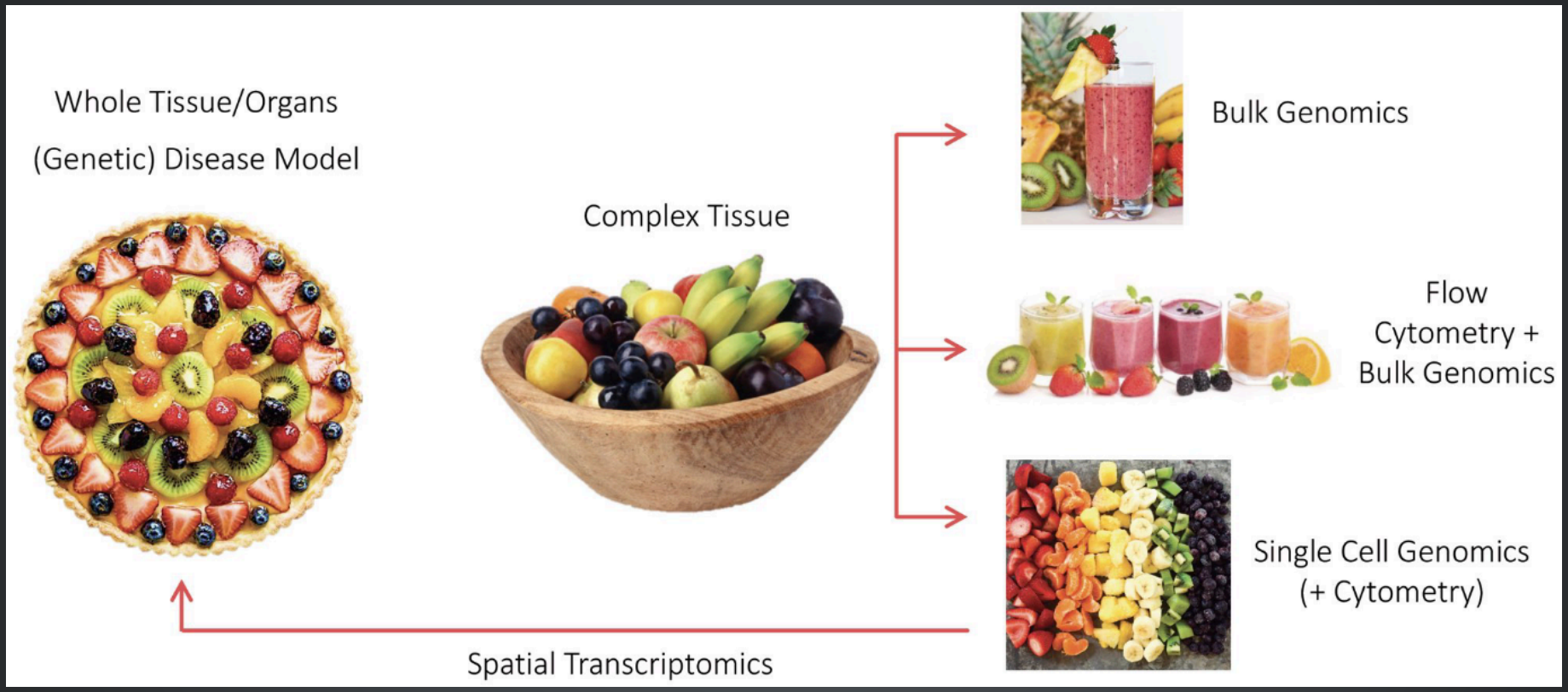

Understanding the complexity of tissue with bulk RNA-seq, scRNA-seq, and spatial transcriptomics.

Spatial Transcriptomics Maps Gene Expression in Tissue

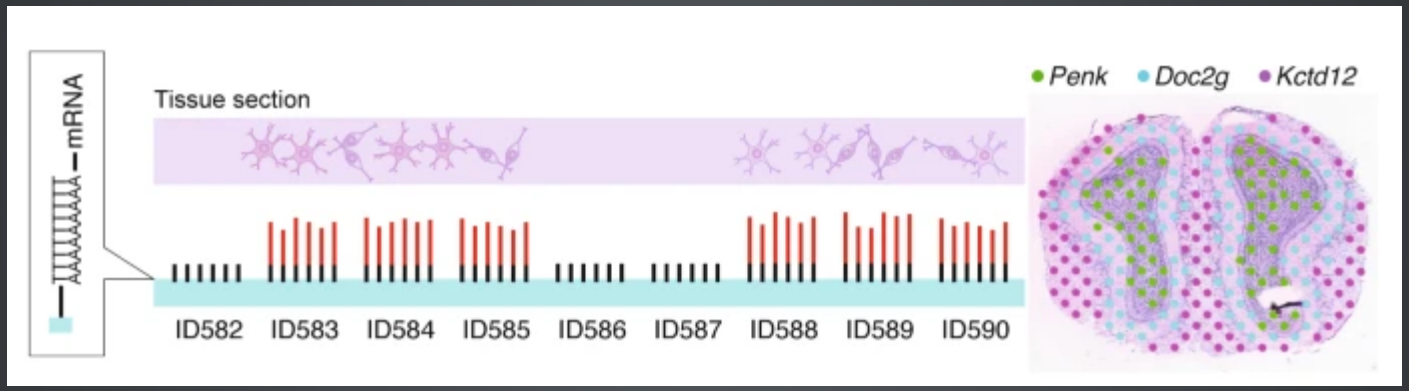

Spatial transcriptomics combines the spatial information of tissue sections with the gene expression data from RNA sequencing.

Example: Mouse Hippocampus in 10x Visium

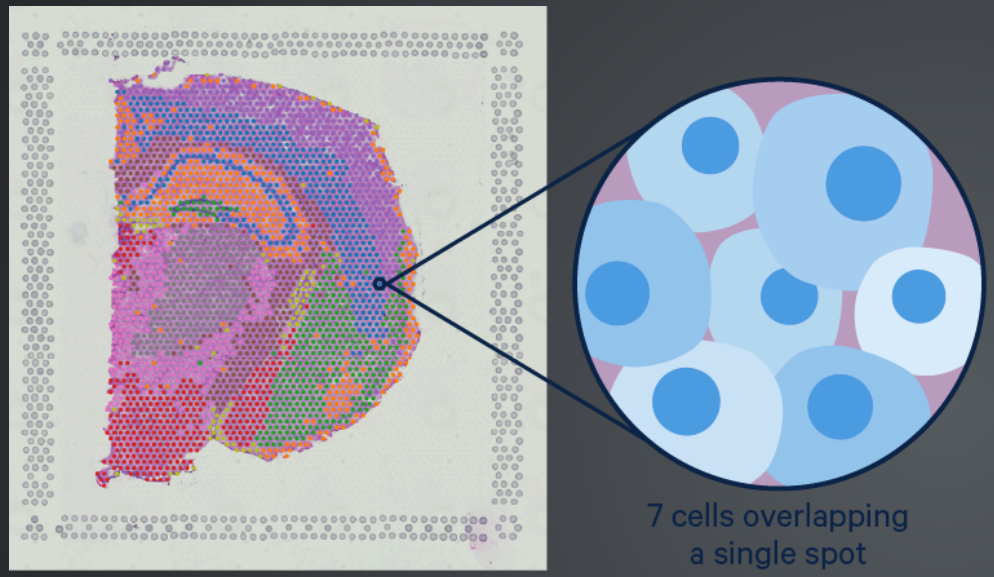

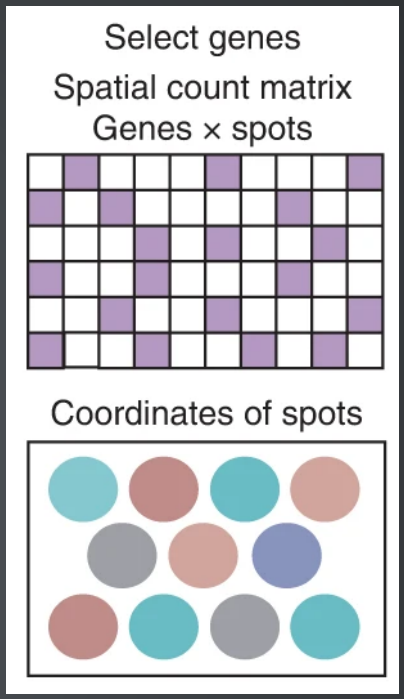

Each spot may contain multiple cells or cell types.

Gene expression matrix is highly sparse count data.

The size of the spots in Visium does not allow us to study gene expression in individual cells. With mixed cell types in spots, we cannot directly map the cell types to the spots.

Deconvolution

Mapping scRNA-seq to Spatial Transcriptomics

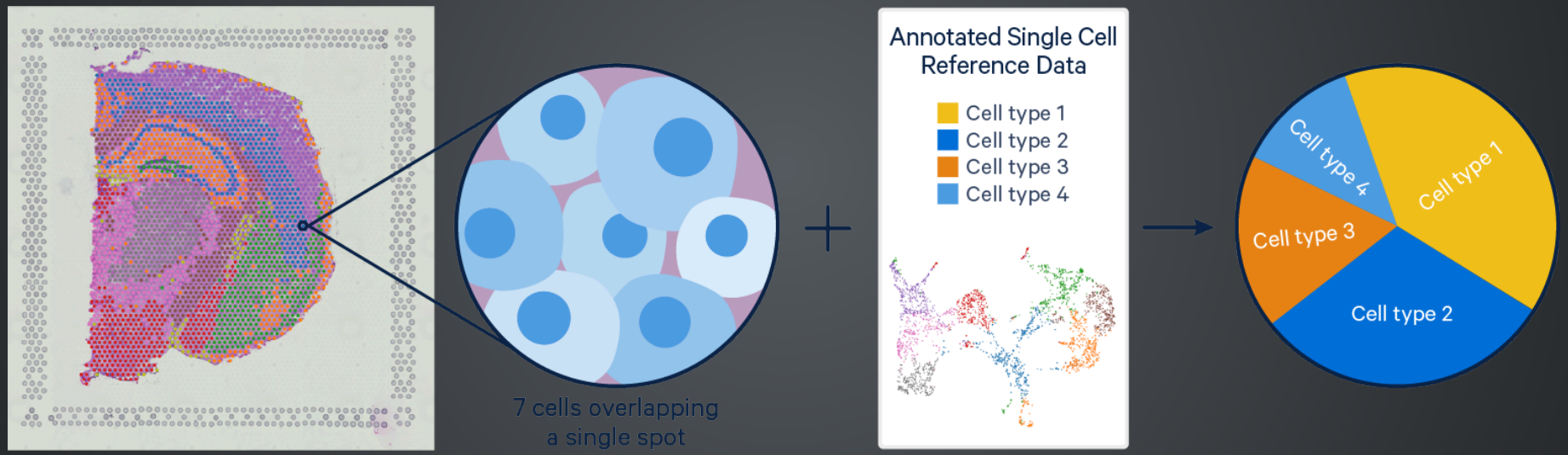

With the reference scRNA-seq data, we can estimate the cell type composition in each spot of the spatial transcriptomics data.

Single-Cell RNA Sequencing (scRNA-seq)

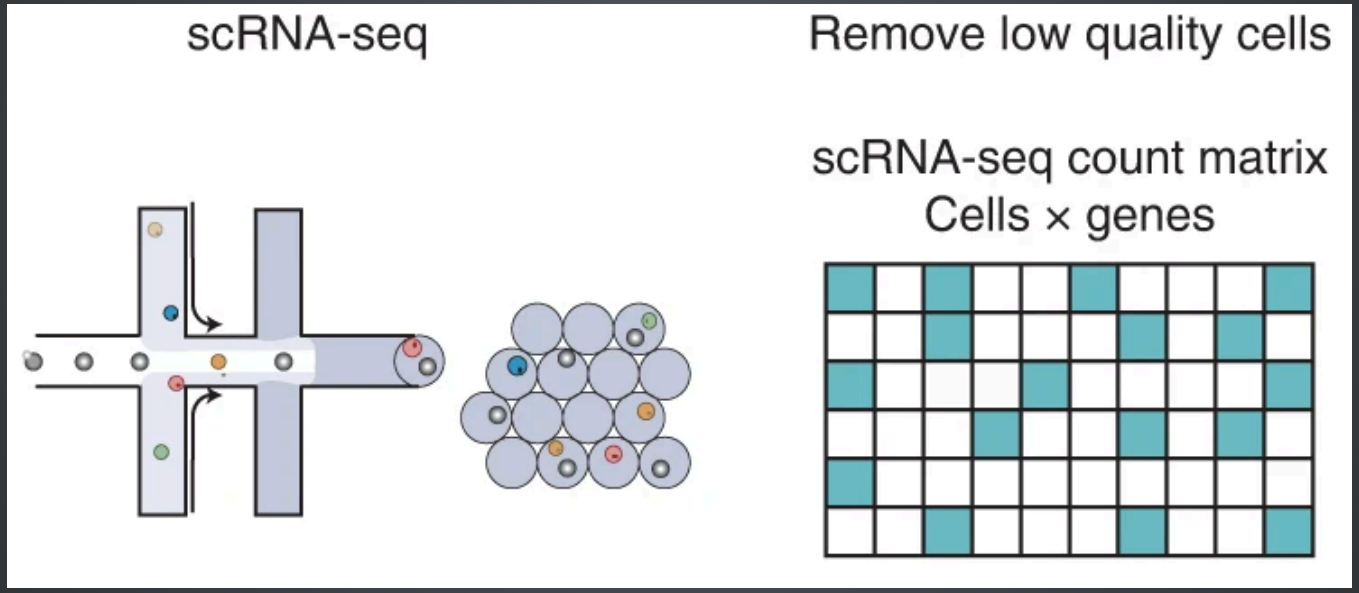

ScRNA-seq data provides the gene expression profile of individual cells, which is also sparse count data.

Compare scRNA-seq with Spatial Transcriptomics

- **Spatial transcriptomics**:
  - Spatial information
  - Typically low cellular resolution
  - Sequence depth is limited
- **ScRNA-seq**:
  - Single-cell resolution
  - High sequence depth

Insights from Deconvolution Results

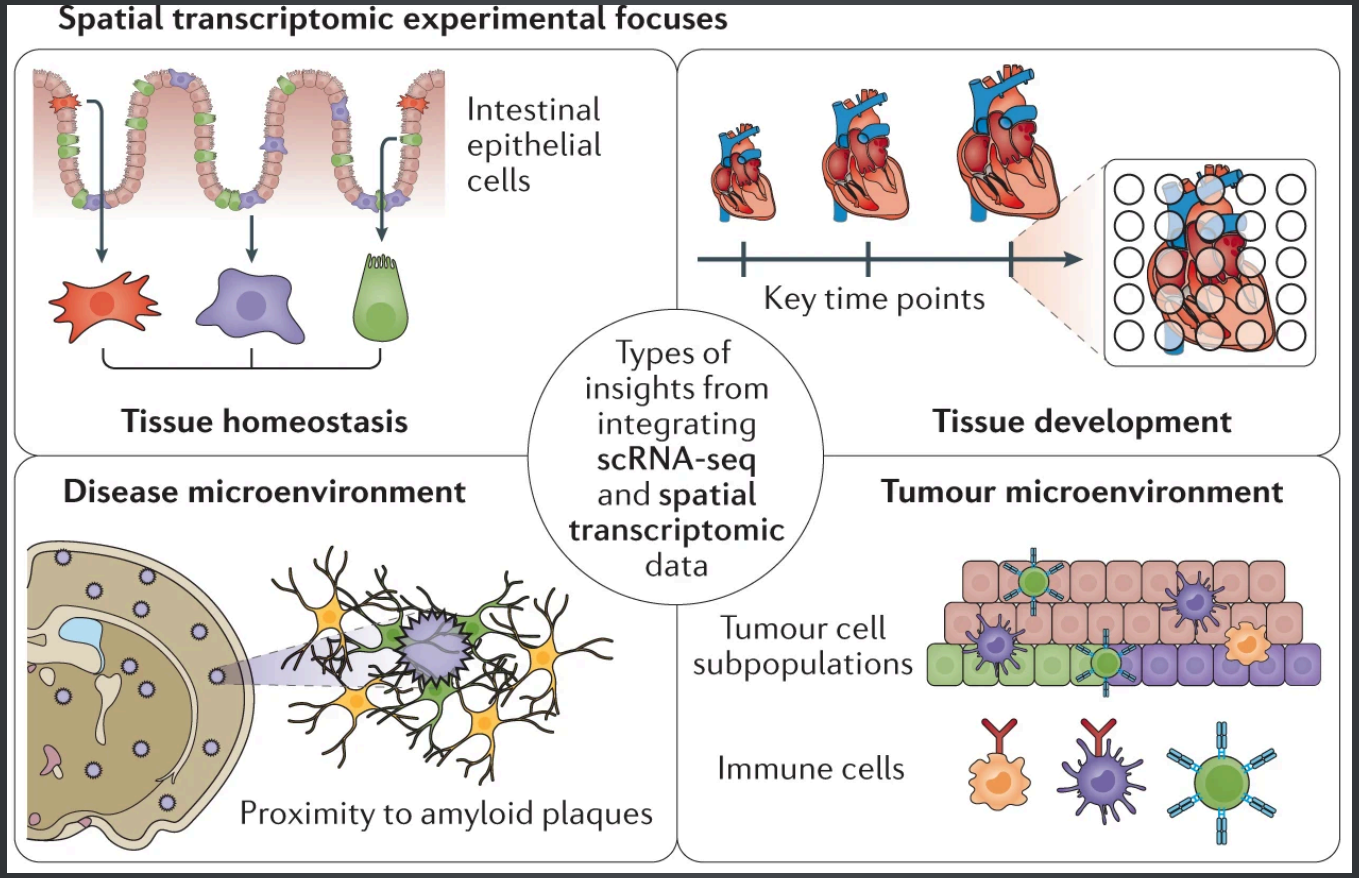

ScRNA-seq and spatial transcriptomics data increase our understanding of the roles of specific cell subpopulations and their interactions in development, homeostasis, and disease.

Deconvolution Methods

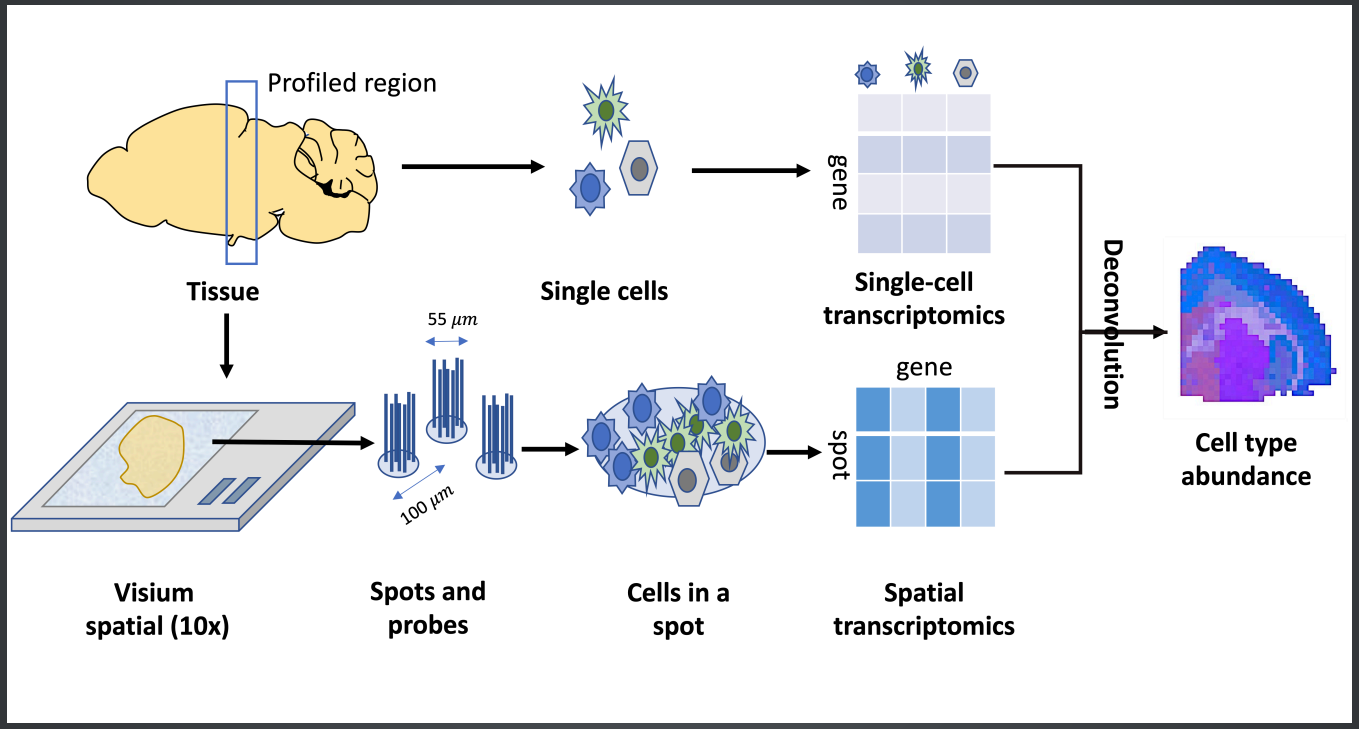

Workflow of deconvolution. Up: discovery of cell types in scRNA-seq data. Down: discovery of gene expression in spatial transcriptomics data.

RCTD: Robust Cell Type Deconvolution

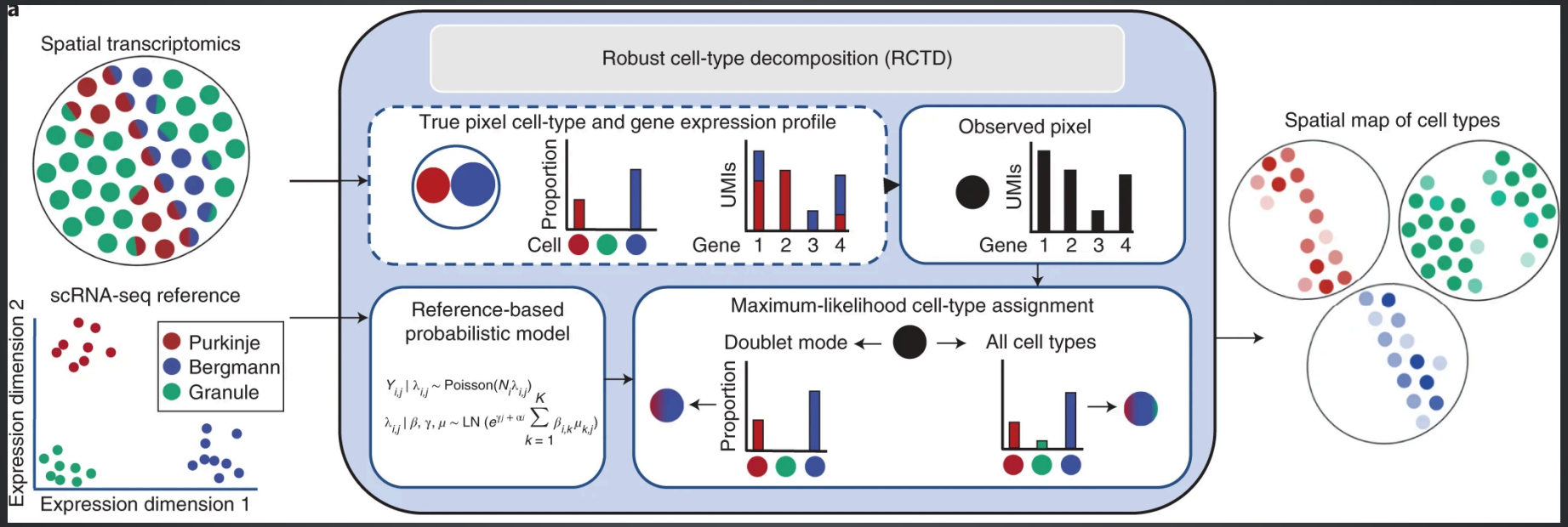

Illustration of the RCTD method

RCTD Notation of Indexing:

- s: index of the spot in spatial transcriptomics dataset
- g: index of the gene
- f: index of the cell type

RCTD Notation of Dataset:

Observed data:

- d_{sg}: observed gene expression count in spot s for gene g
- y_s: total transcript count in spot s, equals to $\sum_g d_{sg}$
- g_{fg}: mean gene expression for gene g in cell type f

RCTD Model

$$d_{sg}|\lambda_{sg} \sim \text{Poisson}(y_s \lambda_{sg})$$
$$\log(\lambda_{sg}) = \alpha_s + \log(\sum_f w_{sf} g_{fg}) + m_g + \epsilon_{sg}$$

Goal: estimate w_{sf} with g_{fg} estimated from scRNA-seq data.

RCTD Notation of Dataset:

Unknown parameters:

- w_{sf}: proportion of cell type f in spot s. $\sum_f w_{sf} = 1$ and $w_{sf} \geq 0$
- λ_{sg}: parameter of the Poisson distribution for gene g in spot s.
- α_s: fixed pixel-specific effect for spot s
- m_g: gene-specific platform random effect for gene g
- ϵ_{sg}: residual error term for gene g in spot s

RCTD Prior Settings

- $m_g \sim \text{Normal}(0, \sigma_m^2)$
- $\epsilon_{sg} \sim \text{Normal}(0, \sigma_\epsilon^2)$.

RCTD Model Fitting

1. **Estimate mean gene expression** g_{fg} from scRNA-seq data, denoted as $\hat{g}_{fg}$.
2.

RCTD Model Fitting

1. **Estimate mean gene expression** g_{fg} from scRNA-seq data, denoted as $\hat{g}_{fg}$.
2. **Gene filtering** Filter out uninformative genes based on $\hat{g}_{fg}$. Reduce to about 3k genes.

RCTD Model Fitting

3. **Platform effect normalization** Estimate m_g for gene g by summarizing the spatial transcriptomics as a single pseudo-bulk measurement $S_g \equiv \sum_s d_{sg} \sim \text{Poisson}(\bar{d}_g)$ with

$$\begin{aligned}\log(\mathbb{E}[\bar{d}_g]|\lambda_{.g}) &= \log\left(\frac{1}{S}\sum_s y_s \lambda_{sg}\right) \\ &= m_g + \log(\bar{y}\sum_f B_{fg} g_{fg}) \\ &\approx m_g + \log(\bar{y}\sum_f w_f g_{fg}) + \log(w_0)\end{aligned}$$

where $B_{fg} = \frac{1}{S}\sum_s \frac{y_s}{\bar{y}} w_{sf} \exp(\alpha_s + \epsilon_{sg})$ and $w_f = \frac{1}{S}\sum_s \frac{y_s}{\bar{y}} w_{sf}\alpha_s$. Obtain the MLE of unknown parameters (w_f, w_0, σ_m^2) and solve for m_g. Denote the predicted platform effect as $\hat{m}_g$.

RCTD Model Fitting

4. **Inference** Estimate w_{sf}, α_s and σ_ϵ^2 by MLE. Assume estimated $\hat{g}_{fg}$ and $\hat{m}_g$ are fixed.
5.

RCTD Model Fitting

4. **Inference** Estimate w_{sf}, α_s and σ_ϵ^2 by MLE. Assume estimated $\hat{g}_{fg}$ and $\hat{m}_g$ are fixed.

5. **Expected cell-type-specific gene expression**
$$\mathbb{E}[d_{sf}|w, d_{sg}] = \frac{d_{sg} w_{sf} \hat{g}_{fg}}{\sum_{f'} w_{sf'} \hat{g}_{f'g}}.$$

RCTD Model Selection

- **Doublet mode** Assigns 1-2 cell types per spot and is recommended for technologies with high spatial resolution such as **Slide-seq** and **MERFISH**.
-
-

RCTD Model Selection

- **Doublet mode** Assigns 1-2 cell types per spot and is recommended for technologies with high spatial resolution such as **Slide-seq** and **MERFISH**.
- **Full mode** Assigns any number of cell types per spot and is recommended for technologies with poor spatial resolution such as **100-micron resolution Visium**.
-

RCTD Model Selection

- **Doublet mode** Assigns 1-2 cell types per spot and is recommended for technologies with high spatial resolution such as **Slide-seq** and **MERFISH**.
- **Full mode** Assigns any number of cell types per spot and is recommended for technologies with poor spatial resolution such as **100-micron resolution Visium**.
- **Multi mode** is an extension of doublet mode that can discover more than two cell types (up to a pre-specified amount) per spot as an alternative option to full mode.

Cell Type Identification by Model Selection

Denote $\mathcal{L}(f)$ as the likelihood of the model with only f th cell type and $\mathcal{L}(f, f')$ as the likelihood of the model only with fth and f'th cell types. For each spot s:

$$\hat{f} = \arg\max_{f} \mathcal{L}(f) \quad \text{and} \quad \hat{f}' = \arg\max_{f' \neq \hat{f}} \mathcal{L}(\hat{f}, f')$$

Cell Type Identification by Model Selection

Because we expect many pixels to be single cell types, we can apply a **penalized approach similar to AIC** to decide between the two models. We select the model maximizing:

$$\mathrm{AIC}(\mathcal{M}) \equiv \mathcal{L}(\mathcal{M}) - V_p(\mathcal{M})$$

where p represents the number of parameters (cell types) and V represents the penalty weight. Select $V = 25$ based on simulation studies.

Confident and Unconfident Spots

Condition: Existence of another pair of cell types (f, f') (f can be equal to f') such that

$$|\mathcal{L}(\hat{f}, \hat{f}') - \mathcal{L}(f, f')| < \delta$$

If the condition holds, the spot is **unconfident**, else it is **confident**.

Sequential Quadratic Programming for MLE

Aim: Convert nonlinear problems into a series of quadratic programming (QP) problems.

The parameter α_s effectively allows us to rescale w_s, so we define $w_{f,s} = w_{f,s}e^{\alpha_s}$, which **will not be constrained to sum to 1**. Next, define:

$$\bar{\lambda}_{s,g}(w_s) = y_s \sum_{f=1}^{F} w_{f,s} g_{f,g} e^{\hat{m}_g} = y_s \sum_{f=1}^{F} w_{f,s} \bar{g}_{f,g}$$

We will refer to this as the predicted mean of gene g in pixel s.

SQP for MLE (cont.)

The final model is a Poisson log-normal mixture model:

$$d_{s,g} \mid \bar{\lambda}_{s,g} \sim \text{Poisson}\left(e^{\varepsilon_{s,g}} \bar{\lambda}_{s,g}\left(w_s\right)\right), \quad \varepsilon_{s,g} \sim \text{Normal}\left(0, \sigma_{\varepsilon}^2\right)$$

We estimate $w_s^* \geq 0$ as the solution that maximizes the **log-likelihood** $\mathcal{L}\left(w_s\right)$:

$$\max \mathcal{L}\left(w_s\right) = \sum_{g=1}^{G} \log P\left(d_{s,g} \mid \bar{\lambda}_{s,g}\left(w_s\right)\right) \quad \text{subject to: } w \geq 0$$

SQP for MLE (cont.)

From now on, we consider a fixed spot s and suppress the notation of s. We will estimate $w^* \geq 0$ as that which maximizes the **log-likelihood** $\mathcal{L}(w)$:

$$\max_w \mathcal{L}(w) = \sum_{g=1}^{G} \log P\left(d_g \mid \lambda_g(w)\right) = \sum_{g=1}^{G} \log Q_{d_g}\left(\lambda_g(w)\right)$$

SQP for MLE (cont.)

Our log likelihood is non-convex. To optimize it, we will apply Sequential Quadratic Programming, an iterative procedure that will be repeated until convergence. Let w_0 be the value of w at a given iteration, and let the gradient of $-\mathcal{L}$ be $b(w)$ and the Hessian of $-\mathcal{L}$ be $A(w)$. Then, we can make the following quadratic Taylor approximation to $\mathcal{L}$:

$$\begin{aligned} -\mathcal{L}(w) \approx & -\mathcal{L}\left(w_0\right)+b(w_0)^T\left(w-w_0\right) \\ & +\frac{1}{2}(w-w_0)^T A\left(w_0\right)\left(w-w_0\right) \end{aligned}$$

SQP for MLE: Construct Positive Semi-Definite Hessian

This QP will not be well-behaved if the Hessian $A\left(w_0\right)$ is not positive semi-definite, which can occur due to the non-convexity of $-\mathcal{L}(w)$. Specifically, suppose we have an eigen-decomposition of H as:

$$H = VDV^T$$

Here, D is a diagonal matrix of eigenvalues. We obtain the positive semi-definite part of H by taking $D^+ = \max(D, 0)$ and:

$$A = VD^+V^T$$

Advantages of RCTD

- Models platform effects by taking spatial transcriptomics as a pseudo-bulk measurement.
- Robust to varying UMI counts per pixel, multiple cell types per pixel, and missing cell types in the reference.

Platform Effect Estimation

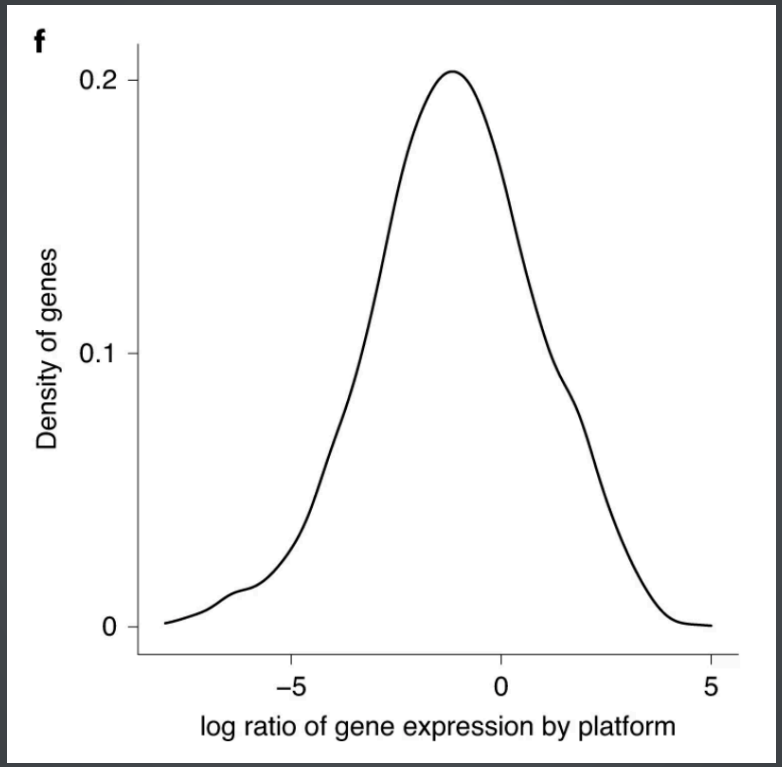

Density plot across genes of measured platform effects between cerebellum **scRNA-seq** and **snRNA-seq** data.

Platform Effect Estimation

In the 3rd step of model fitting, RCTD estimates the platform effect of each gene to transfer cell type information from scRNA-seq to spatial transcriptomics by taking the spatial transcriptomics as a bulk measurement.

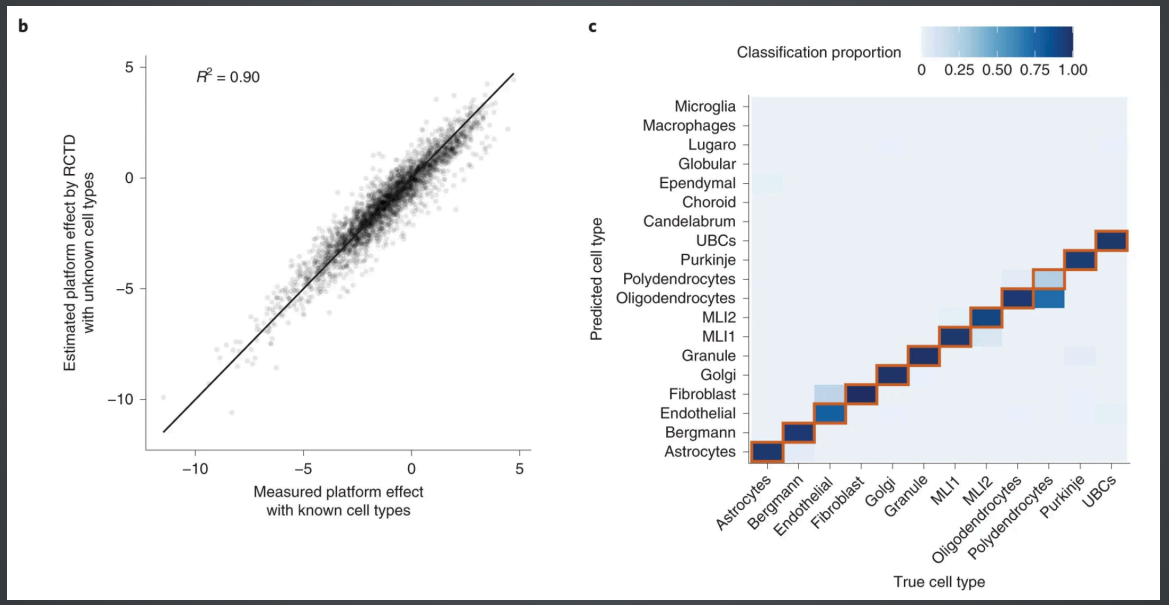

Left: Scatter plot of measured versus predicted platform effect for each gene between the sc and sn cerebellum datasets. Right: Confusion matrix for RCTD's performance on cross-platform (trained on snRNA-seq data and tested on scRNA-seq data).

Robustness

- **Varying unique molecular identifier (UMI) counts per pixel:** Additional UMIs per pixel lead to an increased confidence rate.
-
-

Robustness

- **Varying unique molecular identifier (UMI) counts per pixel:** Additional UMIs per pixel lead to an increased confidence rate.
- **Multiple cell types per pixel:** RCTD was able to accurately predict cell class proportions on pixels containing three or four cell types.
-

Robustness

- **Varying unique molecular identifier (UMI) counts per pixel:** Additional UMIs per pixel lead to an increased confidence rate.
- **Multiple cell types per pixel:** RCTD was able to accurately predict cell class proportions on pixels containing three or four cell types.
- **Missing cell types in the reference:**When cell types in the simulated spatial data were missing from the reference, RCTD classified pixels as the most transcriptionally similar cell type in the reference if available. When no closest cell type was available in the reference, RCTD predicted cell types with reduced confidence rates but often misclassified such pixels.

Application: Detecting Spatially Variable Genes and Effect of Cellular Environment

Differentiate cell type marker genes from spatially variable genes.

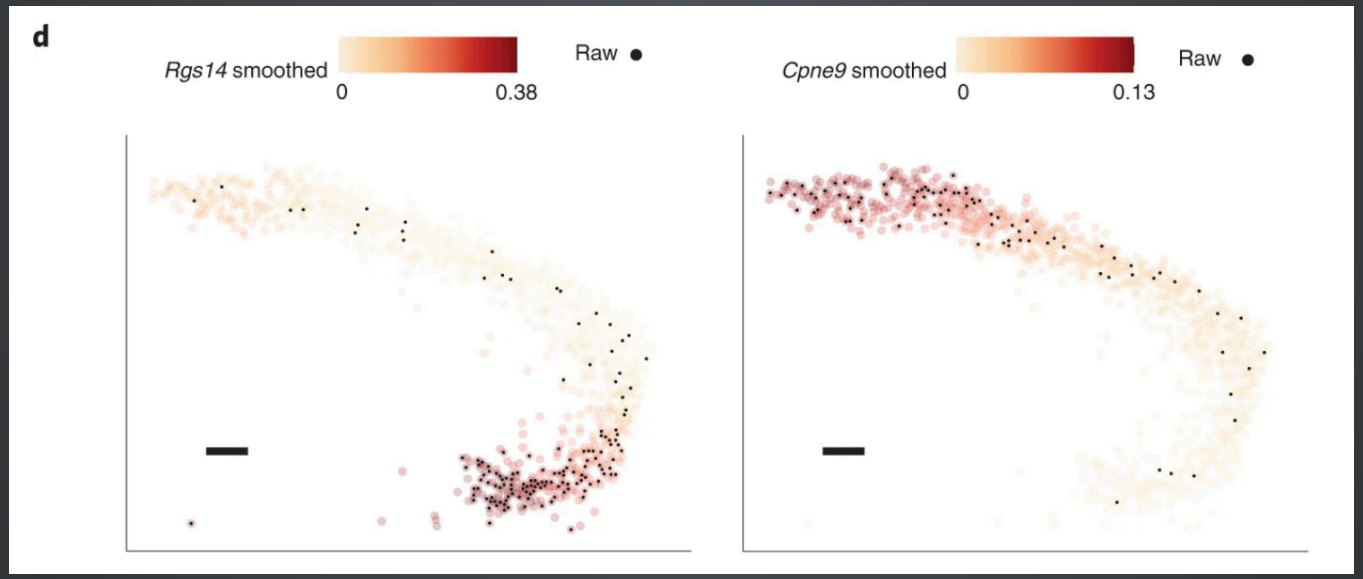

Smoothed spatial expression patterns, recovered by local regression, of two genes detected to have large spatial variation within RCTD's CA3 cells.

Limitations

1. Assumes that platform effects are shared across cell types and random noise ϵ_{fg} is shared across genes.
2. Hard to handle cases when the cell type is missing from the reference but exists in the spatial data.

Cell2Location

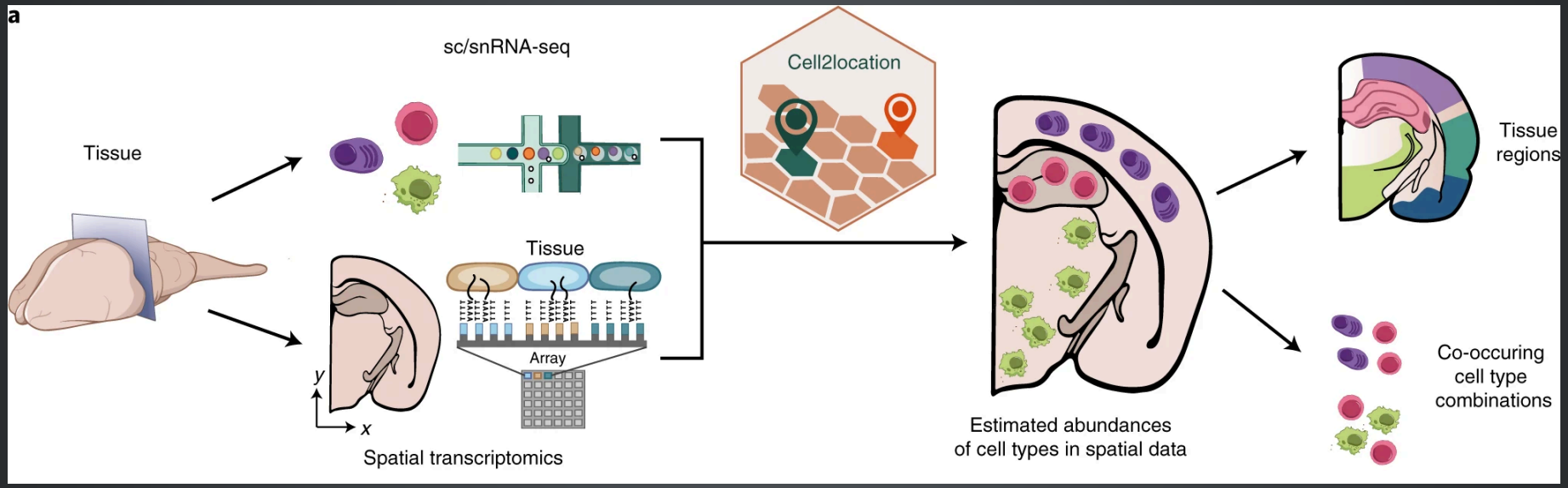

Illustration of the Cell2Location method

Cell2Location Notation of Index

- $g \in \{1, \ldots, G\}$: Gene
- $s \in \{1, \ldots, S\}$: Spot
- $e \in \{1, \ldots, E\}$: Spatial dataset
- $f \in \{1, \ldots, F\}$: Cell type

Cell2Location Notation of Dataset

Input: Matrix of reference expression levels g_{fg} and matrix of spatial expression counts d_{sg}.

Main output: Regression weights w_{sf} which can be transformed into cell type proportions.

Cell2Location Model of mRNA Counts

$$d_{sg} \sim \mathrm{NB}(\mu_{sg}, \alpha_{eg}), \quad \mu_{sg} = \left(m_g \sum_f w_{sf} g_{fg} + s_{eg} \right) y_s$$

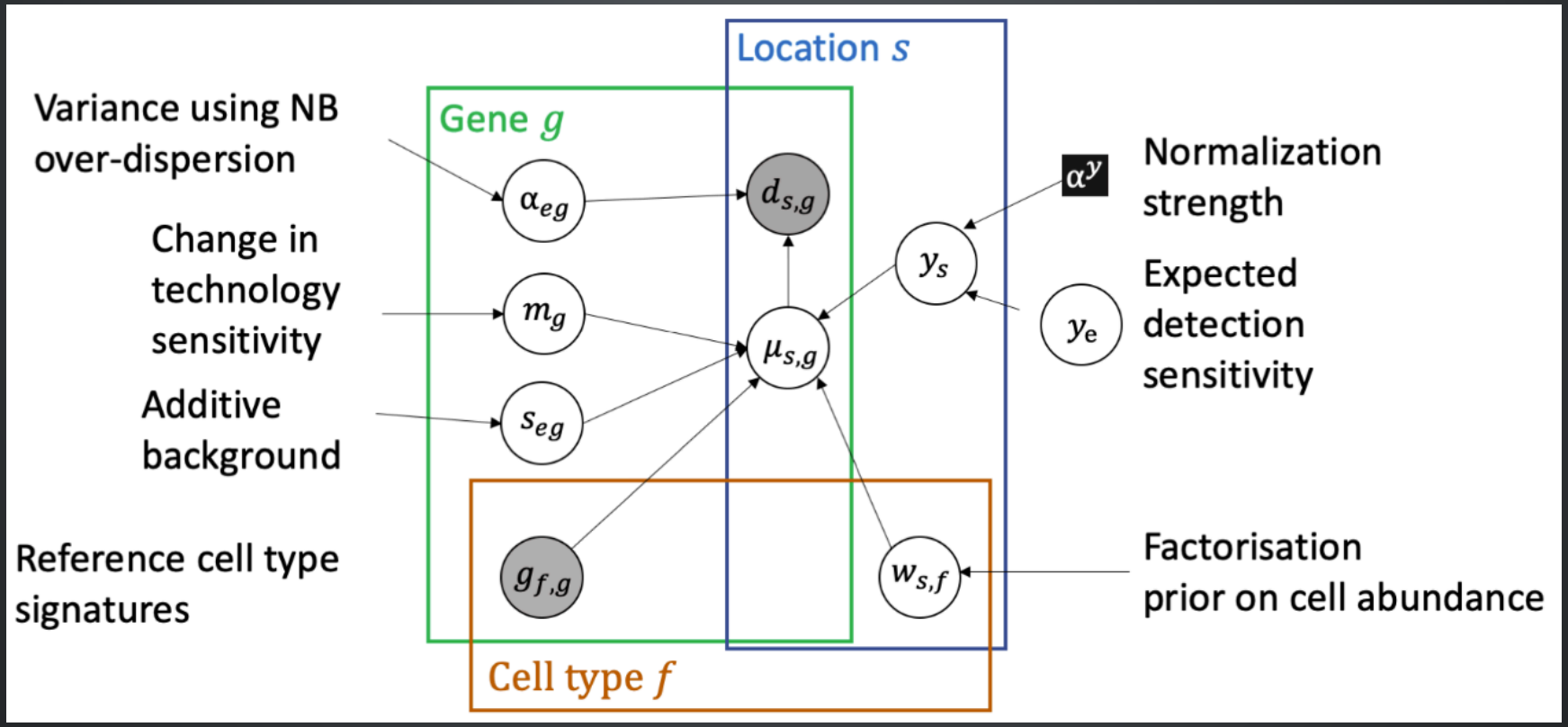

Cell2Location Notation of Model Parameters

- d_{sg}: Spatial expression of gene g in spot s
- μ_{sg}: Unobserved expression level (rate) of gene g in spot s
- α_{eg}: Gene- and batch-specific over-dispersion parameter
- m_g: Technology sensitivity parameter for gene g
- w_{sf}: Regression weight for cell type f in spot s
- g_{fg}: Reference expression level of gene g in cell type f
- s_{eg}: Gene-specific additive shift in spatial dataset e
- y_s: Location-specific scaling factor for spot s

Cell2Location Cell Abundance Prior

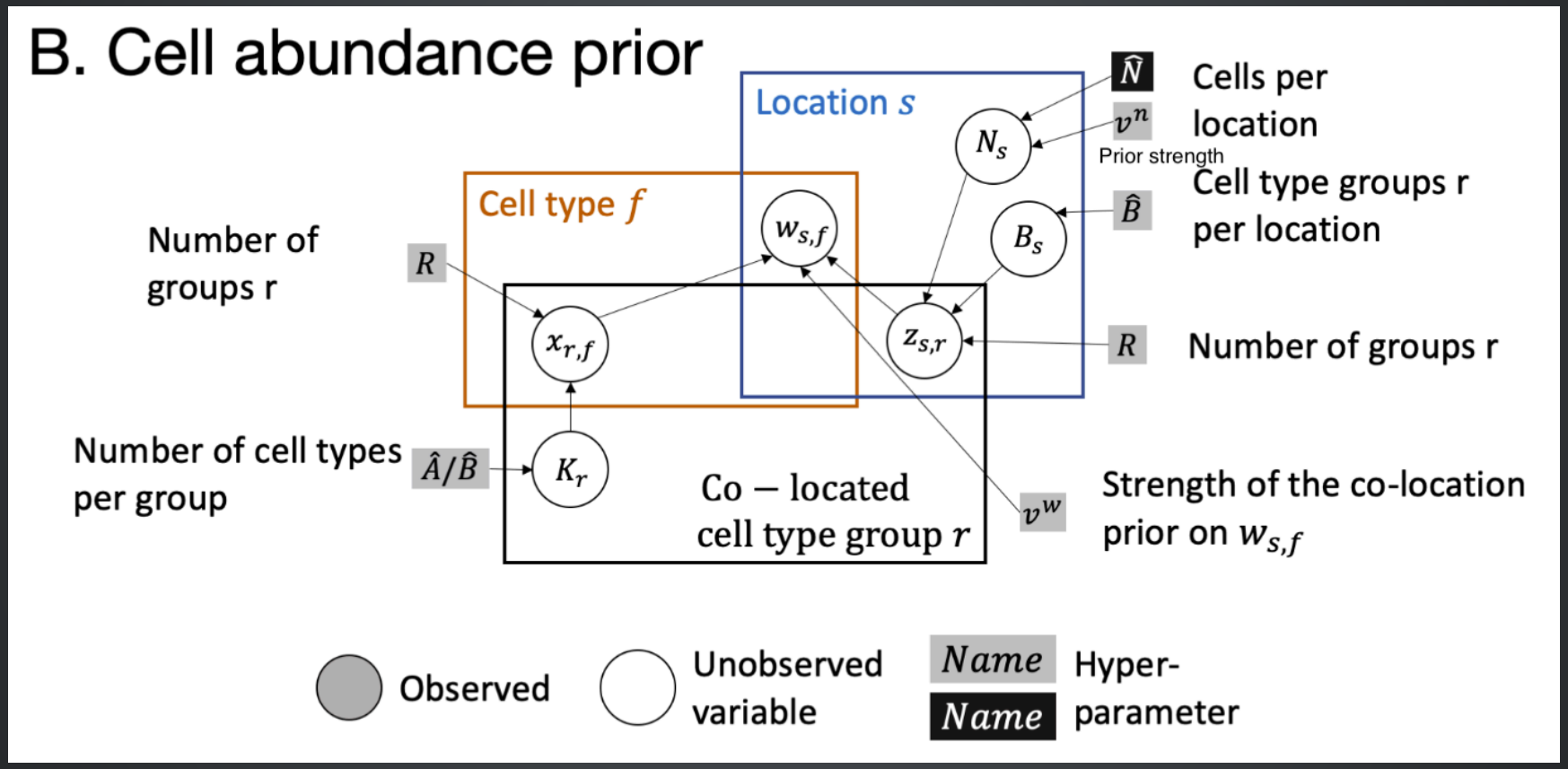

Prior Settings of Cell2Location

Gene-specific multiplicative scaling factor

$$m_g \sim \text{Gamma}\left(\alpha^m, \alpha^m/\mu^m\right) \begin{cases} \alpha^m & = 1/(o^m)^2, \quad o^m \sim \text{Exp}(3) \\ \mu^m & \sim \text{Gamma}(1,1) \end{cases}$$

The prior on detection efficiency per location

$$y_s \sim \text{Gamma}\left(\alpha^y, \alpha^y/y_e\right) \quad y_e \sim \text{Gamma}(10, 10/\mu^y)$$

Overdispersion for each gene

$$\alpha_{eg} = 1/o_{eg}^2, \quad o_{eg} \sim \text{Exp}(\beta^o), \quad \beta^o \sim \text{Gamma}(9,3)$$

Additive shift for genes

$$s_{eg} \sim \text{Gamma}\left(\alpha_e^s, \alpha_e^s/\mu_e^s\right) \begin{cases} \mu_e^s & \sim \text{Gamma}(1, 100) \\ \alpha_e^s & = 1/o_e^2, \quad o_e \sim \text{Exp}(\beta^s), \quad \beta^s \sim \text{Gamma}(9, 3) \end{cases}$$

Cell abundance prior:

$$w_{sf} \sim \text{Gamma}\left(\sum_r z_{sr} x_{rf} \nu^w, \nu^w\right)$$

$$z_{sr} \sim \text{Gamma}\left(B_s/R, 1/(N_s/B_s)\right) \begin{cases} N_s & \sim \text{Gamma}\left(\hat{N}\nu^n, \nu^n\right) \\ B_s & \sim \text{Gamma}\left(\hat{B}, 1\right) \end{cases}$$

$$x_{rf} \sim \text{Gamma}\left(K_r/R, K_r\right), \quad K_r \sim \text{Gamma}\left(\hat{A}/\hat{B}, 1\right)$$

Cell2Location Model: Probabilistic Graph

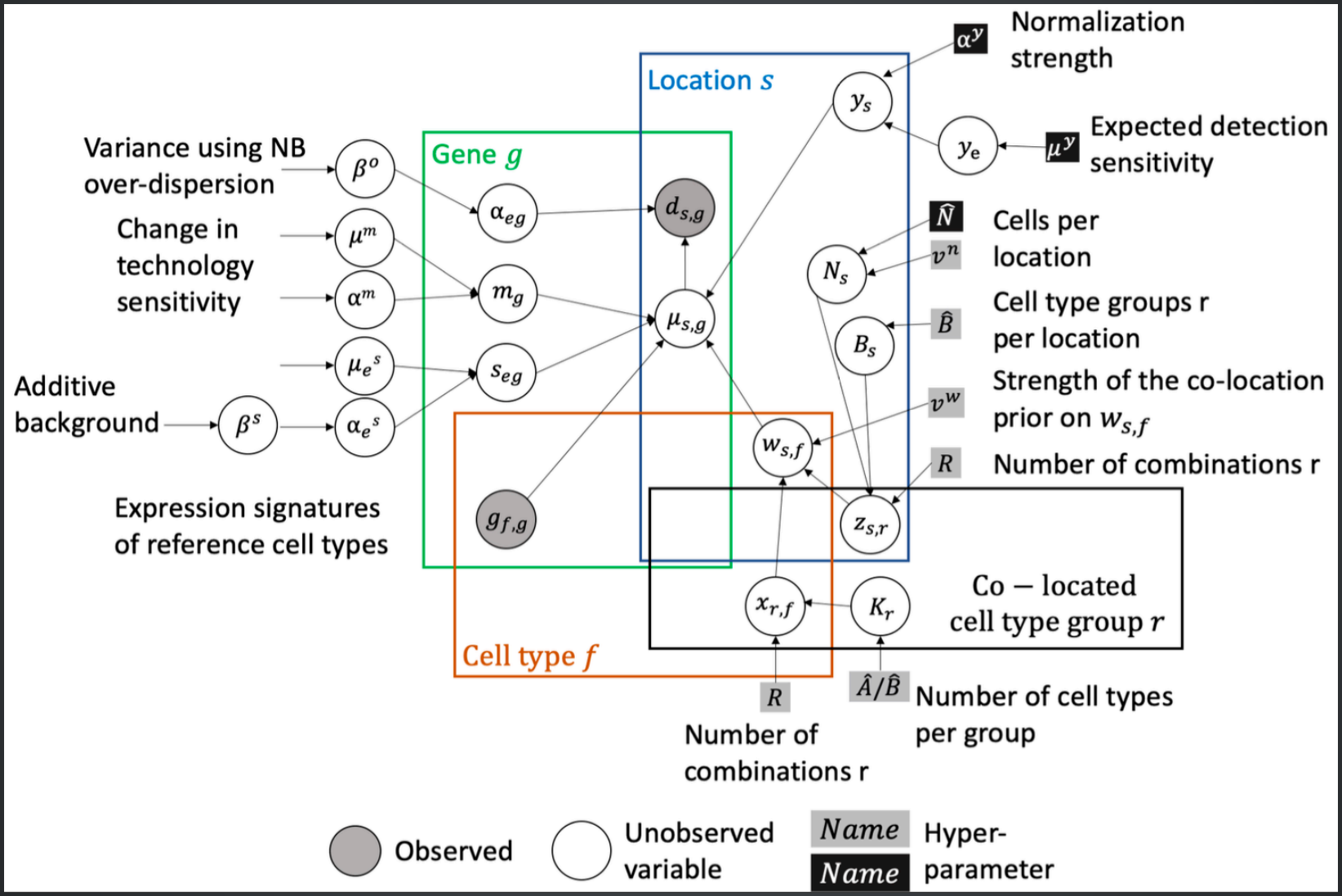

Strength of the Cell2Location Model

Joint modeling of multiple spatial experiments/batches provides several benefits due to normalization and sharing of information between experiments:

-
-
-

Strength of the Cell2Location Model

Joint modeling of multiple spatial experiments/batches provides several benefits due to normalization and sharing of information between experiments:

- Modeling differences in RNA detection sensitivity across experiments: y_e and y_s.
-
-

Strength of the Cell2Location Model

Joint modeling of multiple spatial experiments/batches provides several benefits due to normalization and sharing of information between experiments:

- Modeling differences in RNA detection sensitivity across experiments: y_e and y_s.
- Increasing accuracy by improving the model's ability to distinguish low sensitivity m_g from zero cell abundance w_{rf}.
-

Strength of the Cell2Location Model

Joint modeling of multiple spatial experiments/batches provides several benefits due to normalization and sharing of information between experiments:

- Modeling differences in RNA detection sensitivity across experiments: y_e and y_s.
- Increasing accuracy by improving the model's ability to distinguish low sensitivity m_g from zero cell abundance w_{rf}.
- Increasing sensitivity by sharing factorization prior on cell abundance w_{rf}, namely which cell types tend to co-locate across experiments represented by x_{rf}.

Fitting the Cell2Location Model

Step 1: Construction of Reference Cell Type Signatures

Fitting the Cell2Location Model

Step 1: Construction of Reference Cell Type Signatures

- Distribution: By default, the Cell2Location employs a **negative binomial regression** to estimate reference cell type signatures, which allows robust combination of data from multiple sources.
-

Fitting the Cell2Location Model

Step 1: Construction of Reference Cell Type Signatures

- Distribution: By default, the Cell2Location employs a **negative binomial regression** to estimate reference cell type signatures, which allows robust combination of data from multiple sources.
- Mean: Alternatively, a **hand-coded method** that estimates the average expression of each gene in each cell type can be used.

Fitting the Cell2Location Model

Step 2: Determining the Hyperparameters

-
-

Fitting the Cell2Location Model

Step 2: Determining the Hyperparameters

- Expected cell abundance $\hat{N}$ per location : Can be derived from histology images or tissue type.
-

Fitting the Cell2Location Model

Step 2: Determining the Hyperparameters

- Expected cell abundance $\hat{N}$ per location : Can be derived from histology images or tissue type.
- Hyperparameter α^y for regularizing within-experiment variation in RNA detection sensitivity: If not strong within-experiment variability in RNA detection sensitivity across locations, set $\alpha^y = 200$. Otherwise, set $\alpha^y = 20$.

Fitting the Cell2Location Model

Step 3: Variational Inference

Variational Bayesian Inference is used to approximate the posterior, building on the Automatic Differentiation Variational Inference (ADVI) framework implemented in Pyro.

The posterior distribution over unknown parameters is approximated by softplus-transformed (to ensure a positive scale) univariate normal distributions.

Minimizing the KL divergence between the variational approximation and the true posterior distribution (or maximizing ELBO).

Brief Introduction to Pyro

Here's an example to illustrate the use of Pyro for inference:

```
data = np.random.binomial(1, 0.8, size=200) # random-generated

def model(data): # define the probabilistic model
    # define the hyperparameters that control the Beta prior
    alpha0 = pyro.param("alpha0", torch.tensor(10.0))
    beta0 = pyro.param("beta0", torch.tensor(10.0))
    # sample f from the Beta prior
    f = pyro.sample("latent_var", dist.Beta(alpha0, beta0))
    # sample observed data from the Bernoulli likelihood
    with pyro.plate("data", len(data)):
        pyro.sample("obs", dist.Bernoulli(f), obs=data)

svi = SVI(model,
          AutoDiagonalNormal(model),
          Adam({"lr": 0.0005, "betas": (0.90, 0.999)}),
          loss=Trace_ELBO())

[svi.step(data) for _ in range(1000)] # run inference
```

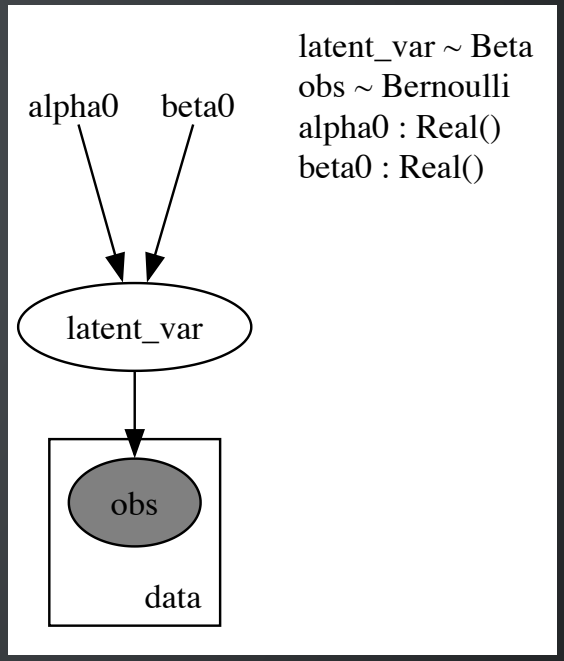

Features of Cell2Location

- Borrow statistical strength across locations with similar cell composition
-
-
-
-

Features of Cell2Location

- **Borrow statistical strength across locations** with similar cell composition
- Account for **batch variation** across slides as well as variation in **mRNA detection sensitivity**
-
-
-

Features of Cell2Location

- Borrow statistical strength across locations with similar cell composition
- Account for batch variation across slides as well as variation in mRNA detection sensitivity
- Estimate absolute cell type abundances by incorporating prior information about the analyzed tissues
-
-

Features of Cell2Location

- Borrow statistical strength across locations with similar cell composition
- Account for batch variation across slides as well as variation in mRNA detection sensitivity
- Estimate absolute cell type abundances by incorporating prior information about the analyzed tissues
- Computationally efficient, owing to variational approximate inference and GPU acceleration
-

Features of Cell2Location

- Borrow statistical strength across locations with similar cell composition
- Account for batch variation across slides as well as variation in mRNA detection sensitivity
- Estimate absolute cell type abundances by incorporating prior information about the analyzed tissues
- Computationally efficient, owing to variational approximate inference and GPU acceleration
- Integrated with the scvi-tools framework and comes with a suite of downstream analysis tools

Sensitivity Analysis of Cell2Location

Cell2Location is sensitive to the choice of α^y and $\hat{N}$ but robust to $\hat{A}$ and $\hat{B}$.

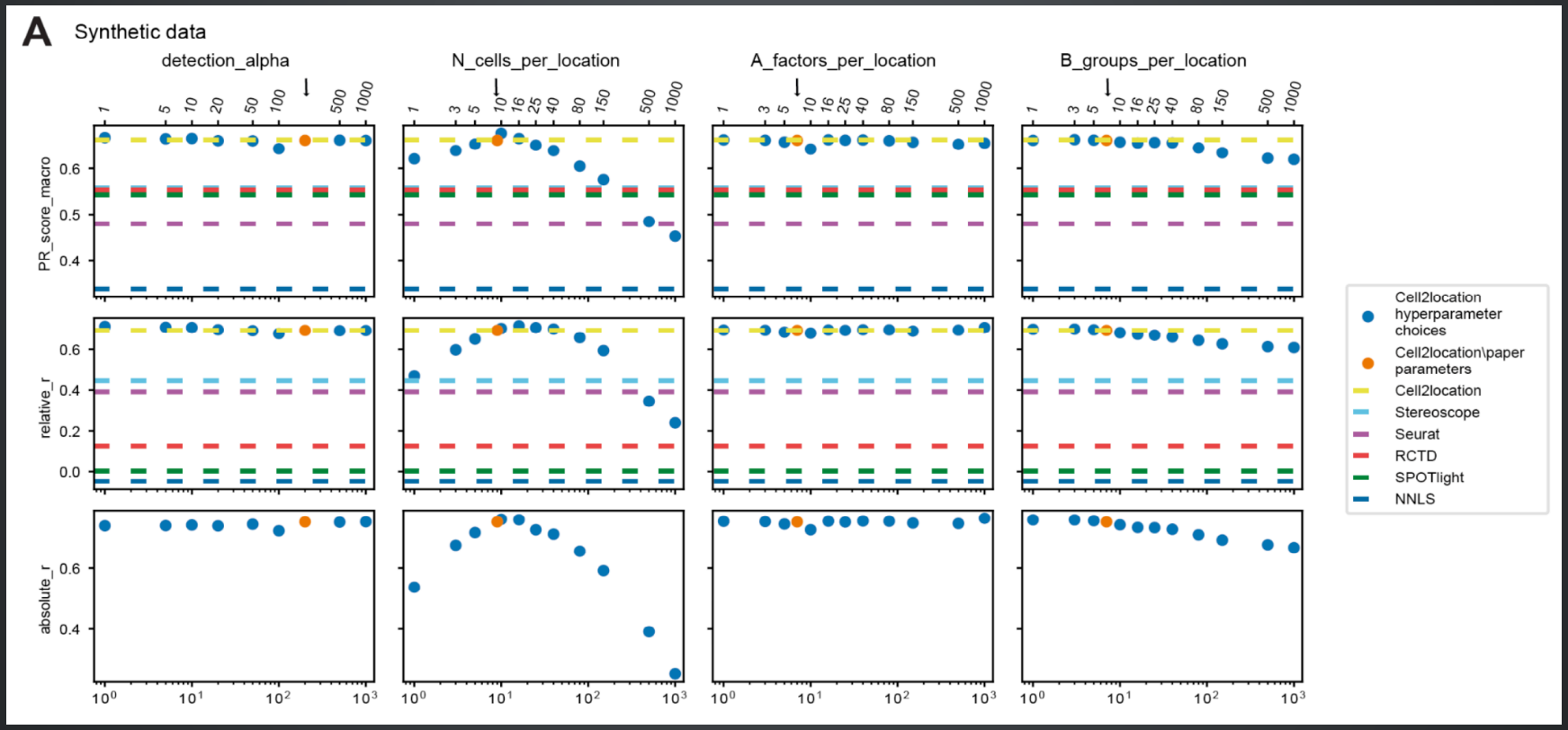

Ablation Study and Unaligned Cell Type Signatures

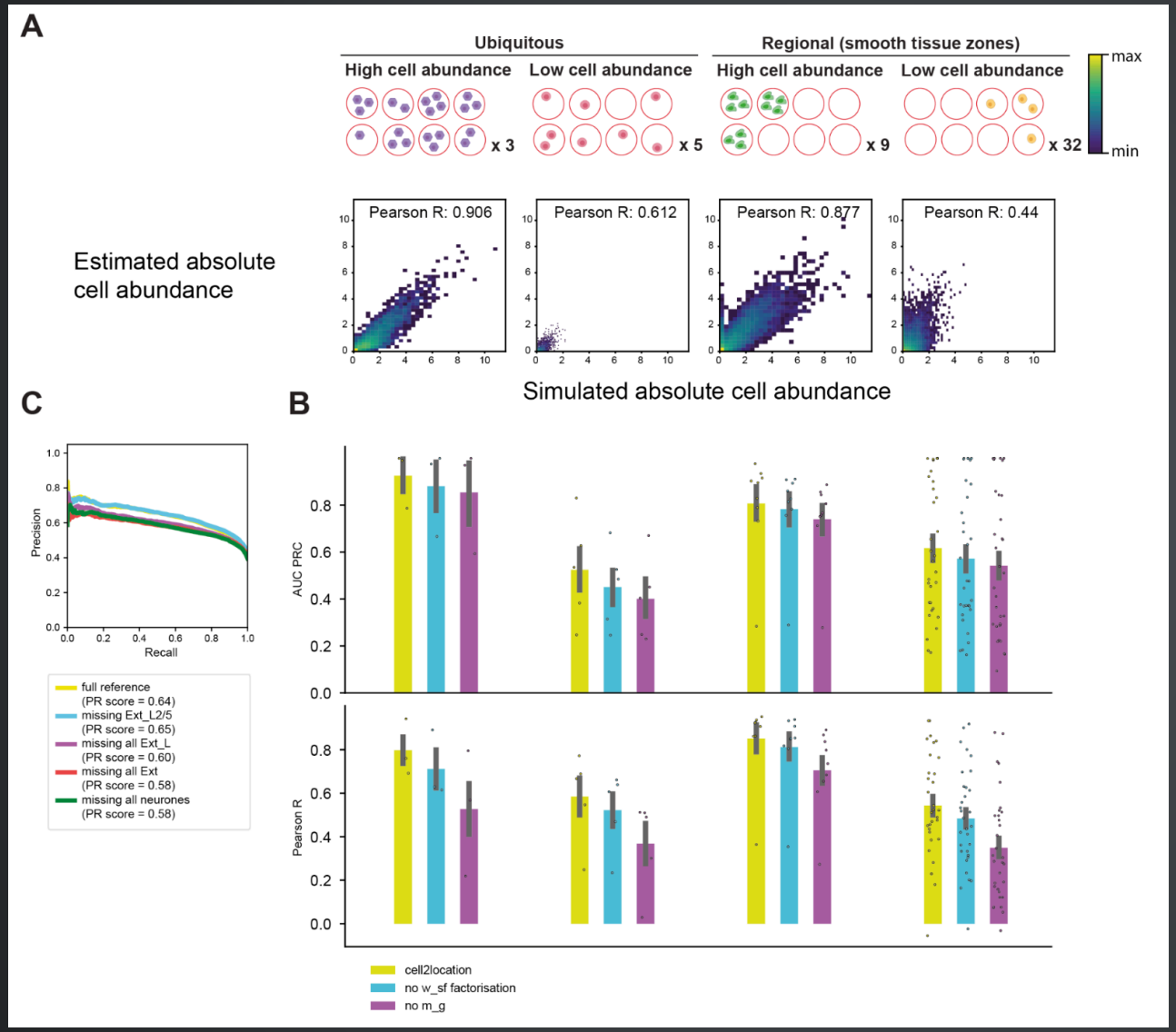

The factorization of the cell type abundance prior w_{sf} and the gene-specific technical sensitivity scaling factor m_g are crucial.

When removing fractions of cell types from the reference signatures, the performance of Cell2Location decreases slightly.

Limitations and Potential Improvements

- Limitations: high computational cost and sensitivity to hyperparameter choices.
- While Cell2Location performs excellently in simulation studies, it competes closely with RCTD in real data analysis.
- Potential improvements: deep learning accelerates tools (e.g., early stopping, learning rate scheduling, etc.) and applying amortized inference.

Accelerating Deep Learning with PyTorch Lightning

PYTORCH

```
# models
encoder = nn.Sequential(nn.Linear(28 * 28, 64), nn.ReLU(), nn.Linear(64, 3))
decoder = nn.Sequential(nn.Linear(3, 64), nn.ReLU(), nn.Linear(64, 28 * 28))

encoder.cuda(0)
decoder.cuda(0)

# download on rank 0 only
if global_rank == 0:
    mnist_train = MNIST(os.getcwd(), train=True, download=True)

# split dataset
transform=transforms.Compose([transforms.ToTensor(),
                              transforms.Normalize(0.5, 0.5)])
mnist_train = MNIST(os.getcwd(), train=True, download=True, transform=transform)

# train (55,000 images), val split (5,000 images)
mnist_train, mnist_val = random_split(mnist_train, [55000, 5000])

# The dataloaders handle shuffling, batching, etc...
mnist_train = DataLoader(mnist_train, batch_size=64)
mnist_val = DataLoader(mnist_val, batch_size=64)

 # optimizer
 params = [encoder.parameters(), decoder.parameters()]
 optimizer = torch.optim.Adam(params, lr=1e-3)

# TRAIN LOOP
model.train()
num_epochs = 1
for epoch in range(num_epochs):
  For train_batch in mnist_train:
    x, y = train_batch
    x = x.cuda(0)
    x = x.view(x.size(0), -1)
    z = encoder(x)
    x_hat = decoder(z)
    loss = F.mse_loss(x_hat, x)
    print('train loss: ', loss.item())

    loss.backward()
    optimizer.step()
    optimizer.zero_grad()

# EVAL LOOP
model.eval()
with torch.no_grad():
  val_loss = []
  for val_batch in mnist_val:
    x, y = val_batch
    x = x.cuda(0)
    x = x.view(x.size(0), -1)
    z = encoder(x)
    x_hat = decoder(z)
    loss = F.mse_loss(x_hat, x)
    val_loss.append(loss)
  val_loss = torch.mean(torch.tensor(val_loss))
  model.train()
```

PYTORCH LIGHTNING

Turn PyTorch into Lightning

Lightning is just plain PyTorch

PyTorch Lightning simplifies deep learning code and accelerates the training process.

Comparison of RCTD and Cell2Location

Modeling, Inference, and Simulation

Model of RCTD and Cell2Location

$$d_{sg}|\lambda_{sg} \sim \text{Poisson}(y_s \lambda_{sg})$$

$$\log(\lambda_{sg}) = \alpha_s + \log(\sum_f w_{sf} g_{fg})$$

$$+ m_g + \epsilon_{sg}$$

RCTD Model

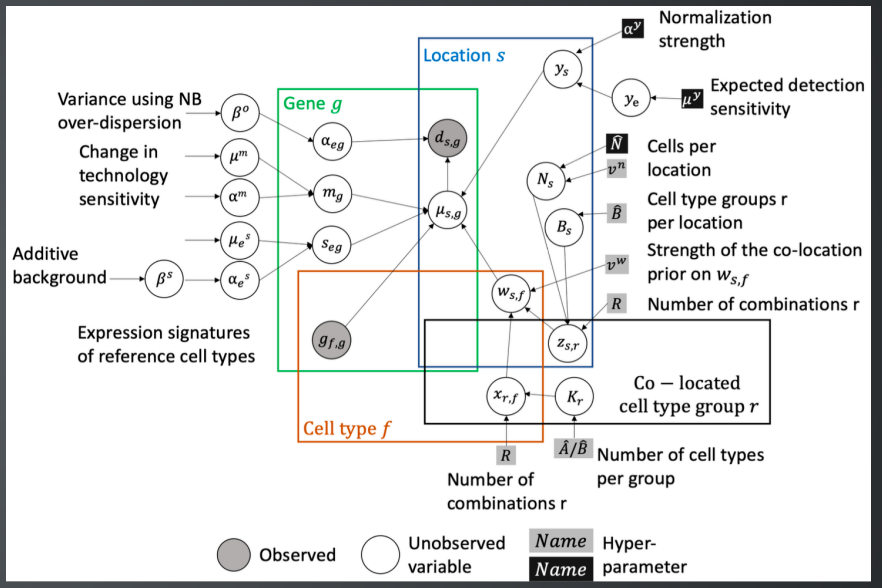

Probabilistic Graph of Cell2Location

Inference Methods

RCTD

Sequential Quadratic Programming for MLE

Convert nonlinear problems into a series of quadratic programming

Cell2Location

Automatic Differentiation Variational Inference

Guide by AutoNormal or Encoder

Programming Language and API

RCTD: R

spacexr

Cell type-specific differential expression with C-SIDE

Cell2Location: Python

scvi-tools / Pyro

Perform many analysis tasks across single-cell, multi, and spatial omics data, e.g., dimensionality reduction, FA, auto-annotation, DE, etc.

Simulation Study

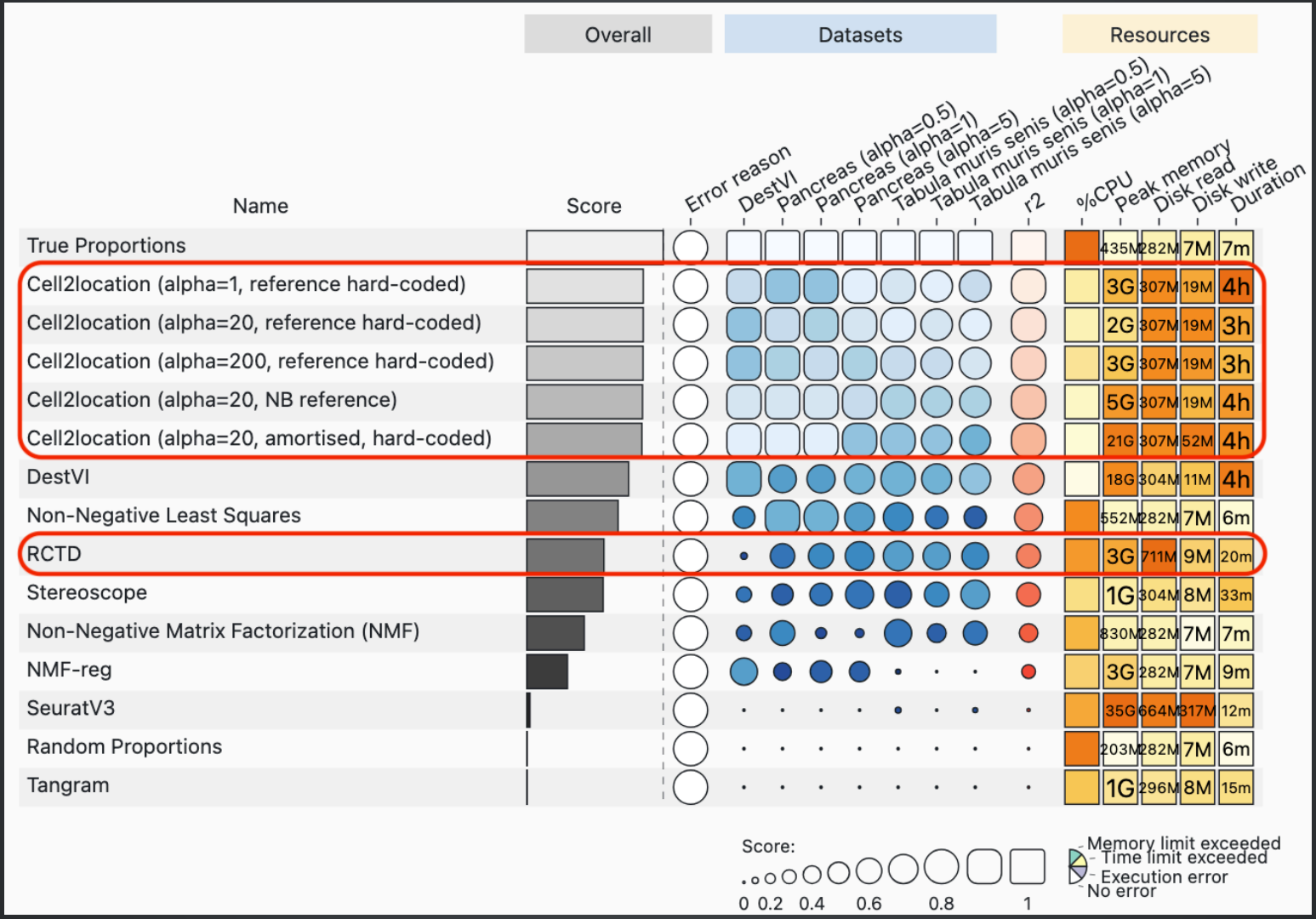

Real Data Analysis: DLPFC

Human DorsoLateral PreFrontal Cortex (DLPFC)

- 10 adult neurotypical controls
- 3 positions: anterior, middle, and posterior
- Annotated snRNA-seq and spatial transcriptomics
- By 10x Genomics Chromium and Visium

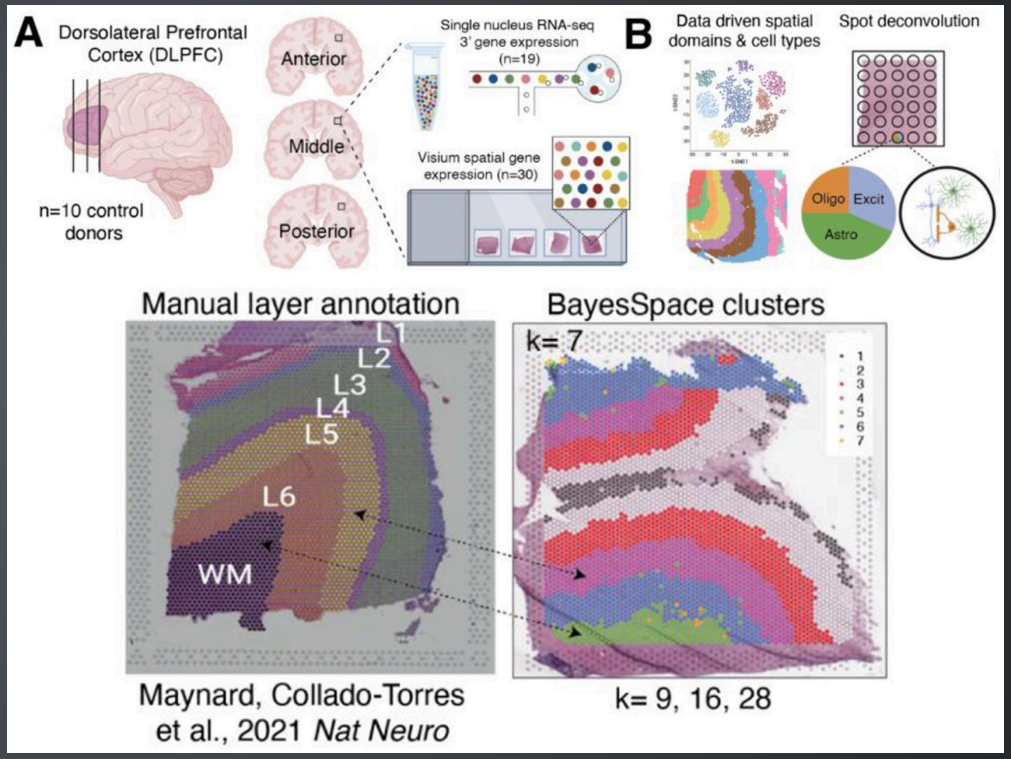

Study design to generate paired single nucleus RNA-sequencing (snRNA-seq) and spatially-resolved transcriptomic data across DLPFC.

Real Data Analysis: Data after QC

QC: Criteria

- Remove cell types with fewer than 25 cells
- Reduce genes according to the minimum average expression and log fold change
- Remove genes appearing in fewer than 10 spots
- Keep genes present in both snRNA-seq and spatial transcriptomics
- Reduce #gene to around 3k

Spatial Transcriptomics

- #Spot: 3639

SnRNA-seq

- #Gene: about 3k
- #Cell: 2k-5k

Real Data Analysis: Layer Level Results

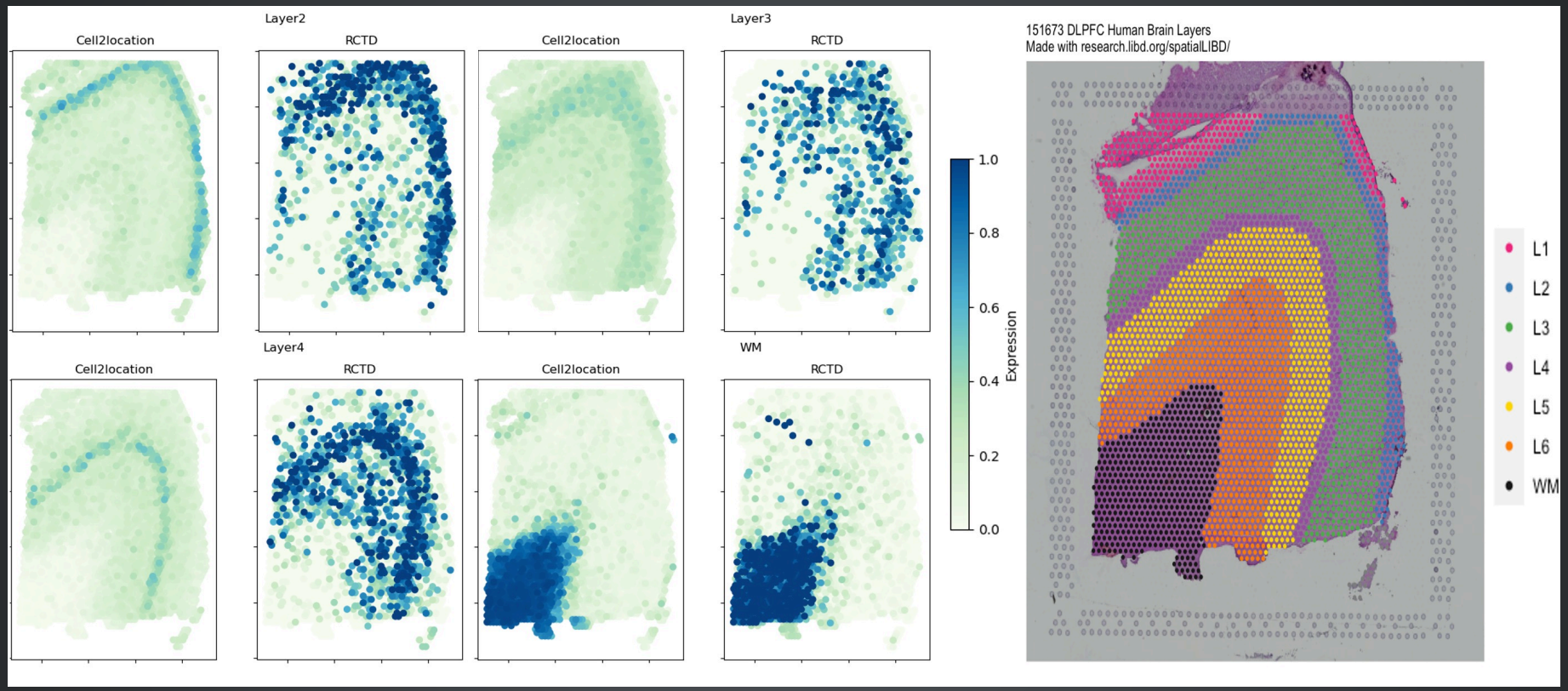

Left panel shows layer level results of two methods in paired DLPFC data. Right panel shows the manual annotation.

Real Data Analysis: Cell Type Level Results

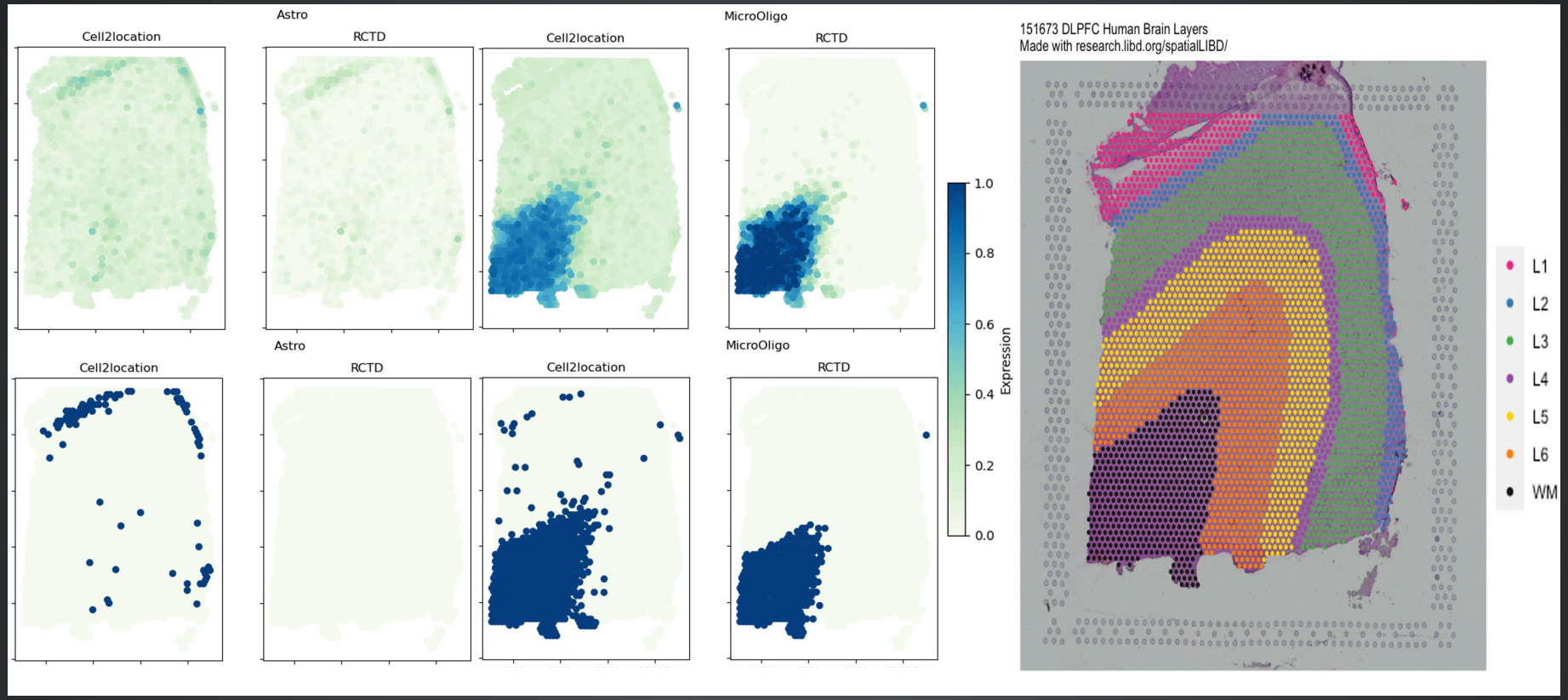

Cell type level results of RCTD and Cell2Location in paired DLPFC data. Manual annotation of two cell types: Astrocytes in layer 1, Micro-Oligodendrocytes in layer 1 as well as white matter. Upper left shows the result of deconvolution visualizing the proportion of a given cell type. Lower left shows the result of mapping assigning spots to the most likely cell type.

Insights from Real Data Analysis

- The runtime of Cell2Location is significantly longer than RCTD. Deep learning-based methods may not converge if the runtime is limited.
- Although Cell2Location may not always converge, its results appear to be more accurate than those of RCTD.
- Compared to RCTD, Cell2Location provides smoother and less noisy results.
- At the layer level, Cell2Location can leverage spatial information regarding the similarity of spots, which may enhance its performance.

References

1. Kleshchevnikov V, Shmatko A, Dann E, et al. Cell2location maps fine-grained cell types in spatial transcriptomics[J]. Nature biotechnology, 2022, 40(5): 661-671. [link]
2. Cable D M, Murray E, Zou L S, et al. Robust decomposition of cell type mixtures in spatial transcriptomics[J]. Nature biotechnology, 2022, 40(4): 517-526. [link]
3. Marx, V. Method of the Year: spatially resolved transcriptomics. Nat Methods 18, 9–14 (2021). [link]
4. Li B, Zhang W, Guo C, et al. Benchmarking spatial and single-cell transcriptomics integration methods for transcript distribution prediction and cell type deconvolution[J]. Nature methods, 2022, 19(6): 662-670.
5. Integrating Single Cell and Visium Spatial Gene Expression Data. 10x Genomics. 2023. [link]
6. Spatial Decomposition. Open Problems in Single-Cell Analysis. 2023. [link]
7. Huuki-Myers L A, Spangler A, Eagles N J, et al. A data-driven single-cell and spatial transcriptomic map of the human prefrontal cortex[J]. Science, 2024, 384(6698): eadh1938. [link]
8. PyTorch Lightning. 2023. [link]